A PROOFS

A.1 Proofs about Probabilistic Filter

A.1.1 Proof of Proposition 3.2.

Proof. Here we prove that $\Pr\left[Q(\phi) \notin \left[l_{\phi,\delta}, r_{\phi,\delta}\right]\right] \leq \delta$. For the failure case of $Q(\phi) < l_{\phi,\delta}$, there is $Q(\phi) < l_{\phi,\delta} \Rightarrow \hat{R}(Q(\phi)) \leq \hat{R}\left(l_{\phi,\delta}\right) \leq \phi \cdot N - t \Rightarrow \hat{R}(Q(\phi)) - R(Q(\phi)) \leq -t$. Similarly, there is $Q(\phi) > r_{\phi,\delta} \Rightarrow \hat{R}(Q(\phi)) - R(Q(\phi)) \leq -t$. Finally we have $Q(\phi) \notin \left[l_{\phi,\delta}, r_{\phi,\delta}\right] \Rightarrow |\hat{R}(Q(\phi)) - R(Q(\phi))| \geq t$ and thus $\Pr\left[Q(\phi) \notin \left[l_{\phi,\delta}, r_{\phi,\delta}\right]\right] \leq \delta$.

□

A.1.2 Proof of Proposition 3.3.

Proof. The proof for $\mathbb{E}[f_\delta]$ is based on $\mathbb{E}\left[\hat{R}(x) - R(x)\right] = 0$ for any value x. According to the Formula 3 of $l_{\phi,\delta}$, $r_{\phi,\delta}$, the filter size is $f_\delta = R(r_{\phi,\delta}) - R(l_{\phi,\delta}) = \hat{R}\left(r_{\phi,\delta}\right) - \hat{R}\left(l_{\phi,\delta}\right) + \left(R(r_{\phi,\delta}) - \hat{R}\left(r_{\phi,\delta}\right)\right) - \left(R(l_{\phi,\delta}) - \hat{R}\left(l_{\phi,\delta}\right)\right)$ and thus $\mathbb{E}[f_\delta] = 2t + 0 - 0 = 2t$.

As for $f_\delta - \mathbb{E}[f_\delta]$, we have

$$f_\delta - \mathbb{E}[f_\delta] = \left(R(r_{\phi,\delta}) - \hat{R}\left(r_{\phi,\delta}\right)\right) - \left(R(l_{\phi,\delta}) - \hat{R}\left(l_{\phi,\delta}\right)\right)$$

$$= \sum_{h=1}^{H} \sum_{i=1}^{m_h} w_h \cdot \left(X_{i,h}(l_{\phi,\delta}) - X_{i,h}(r_{\phi,\delta})\right).$$

Note that if the i-th compaction at height h chooses odd-indexed items there is $X_{i,h}(l_{\phi,\delta}), X_{i,h}(r_{\phi,\delta}) \in \{0, 1\}$, otherwise $X_{i,h}(l_{\phi,\delta}), X_{i,h}(r_{\phi,\delta}) \in \{0, -1\}$. For randomized compaction, it holds that

$$|X_{i,h}(l_{\phi,\delta}) - X_{i,h}(r_{\phi,\delta})| \leq 1,$$

$$\Pr[X_{i,h}(l_{\phi,\delta}) - X_{i,h}(r_{\phi,\delta}) = 0] \geq 0.5,$$

$$\mathbb{E}\left[X_{i,h}(l_{\phi,\delta}) - X_{i,h}(r_{\phi,\delta})\right] = \mathbb{E}\left[X_{i,h}(l_{\phi,\delta})\right] - \mathbb{E}\left[X_{i,h}(r_{\phi,\delta})\right] = 0.$$

Thus we have $\mathbb{E}[f_\delta - \mathbb{E}[f_\delta]] = 0$, $\mathrm{Var}[f_\delta - \mathbb{E}[f_\delta]] \leq \frac{1}{2}\sum_{h=1}^{H-1} m_h w_h^2 = \sigma^2$, and $\mathrm{Var}[f_\delta - \mathbb{E}[f_\delta]]$ is zero-mean σ^2-sub-Gaussian. □

A.2 Proofs about Time Complexity

A.2.1 Proof of Proposition 4.1.

Proof. First, we illustrate the termination of recursive estimation, i.e., the leaf nodes in Figure 9. Note that distribution X is sub-Gaussian and has an upper bound f_0 as shown in Figure 7(b) because $f_\delta \leq f_0$. In other words, $G_{M,\delta}(X)$ is simply 1 when $X \leq f_0 \leq M$, i.e., using a deterministic sketch can end the multi-pass selection in the next pass. In other words, the recursion terminates at G nodes.

In Figure 7(a), all three cases make the number of values less than f_0 while the failure cases incur an extra pass. In other words, a failure means the method takes two passes to shrink the ranges, which is smaller than that after taking a pass with deterministic sketches. If P passes (shrinking value ranges $P-1$ times) are enough for selection with deterministic sketches, $(P-1) * 2 + 1 = 2P - 1$ passes are always sufficient for that with randomized sketches.

□

A.2.2 Proof of Lemma 4.2.

Proof. As shown in Figure 7(a), all the cases make the number of values smaller than f_0 and makes the depth increased by 1 in the recursive tree 9. Let P passes be enough for selection with deterministic sketches, then the depth of the tree will not exceed P and the number of nodes is $O(2^P)$. According to the results in [33], there is $M = O\left(N^{1/P} \cdot (\log N)^2\right)$, i.e., $O(2^P) = O\left(N^{1/\log(M/\log^2 N)}\right)$. □

A.2.3 Proof of Proposition 4.4.

Proof. The m_h under any number of values N' can be computed by simply ingesting N' nulls into a randomized sketch with size limit M. No significant space cost is introduced since the items in the sketch are not maintained. In other words, it is just maintaining the shape of the sketch. As we only focus on m_h, the nulls can be ingested in batches each triggering a compaction.

With the laziness technique in compaction operations [24], i.e., perform compactions only when the sketch size reaches M, each compaction compacts $M/H = \Omega(M/\log N)$ items on average. It takes $O(H) = O(\log N)$ time, since we only need to decide the height to compact and update the shape. Each value contributes $1 + \frac{1}{2} + \frac{1}{4} + \ldots = O(1)$ to the total number of items in compactions, as a sketch item at height h represents 2^{h-1} values. Hence, the complexity of estimation is $O\left(\frac{(N\log^2 N/M)\cdot \log N}{M/\log N}\right) = O\left(N\log^4 N/M^2\right)$.

□

A.3 Proofs about Space Complexity

A.3.1 Proof of Proposition 4.5.

Proof. Following the analysis in mergeable KLL sketch [26], for the sketch summarizing N values in the first pass, let k be the capacity of the top compactor and c be the capacity decrease rate.

We first show that the condition of $\Pr\left[f_{\delta'} \geq N/(\frac{N}{k})^{\frac{1}{P-1}}\right] \leq \delta'$ suffices, where $\delta' = \frac{\delta}{2(P-1)}$. Intuitively, the condition means that choosing δ'-filter in the first pass is likely to shrink the number of values between filters at a rate of $(\frac{N}{k})^{\frac{1}{P-1}}$. In the following passes, choosing δ'-filter can shrink faster, since the sketch is more accurate (fewer values are sketched and the space budget is fixed). Thus after successfully applying δ'-filters $P-1$ times, the filter size is shrunk to at most $N/(\frac{N}{k})^{\frac{1}{P-1}\cdot(P-1)} = k$, i.e., the answer can be determined in the P-th pass. Now we compute the probability of the scenario occurring: The probability of all $P-1$ δ'-filters being correct is at least $(1-\delta')^{P-1}$; The probability of shrinking the number of values between the filter fast enough $P-1$ times is at least $(1-\delta')^{P-1}$. Thus with a probability of at least $((1-\delta')^{P-1})^2 \geq 1 - 2(P-1)\delta' = 1 - \delta$, the quantile is selected after P passes.

Next, we show that $\Pr\left[|X| \geq \frac{1}{3}N/(\frac{N}{k})^{\frac{1}{P-1}}\right] \leq \delta'$ suffices the condition above, where X is a sub-Gaussian variable with variance $\sigma^2 = \frac{1}{2}\sum_{h=1}^{H-1} m_h w_h^2$ (Formula 1) representing the rank error of the sketch. When it holds, there is $t = \frac{1}{3}N/(\frac{N}{k})^{\frac{1}{P-1}}$ (defined in Section 3.1.1) and recall that $\mathbb{E}[f_{\delta'}] = 2t$ (Proposition 3.3). Thus we have $\Pr\left[f_{\delta'} \geq N/(\frac{N}{k})^{\frac{1}{P-1}}\right] = \Pr\left[f_{\delta'} - 2t \geq N/(\frac{N}{k})^{\frac{1}{P-1}} - 2t\right]$

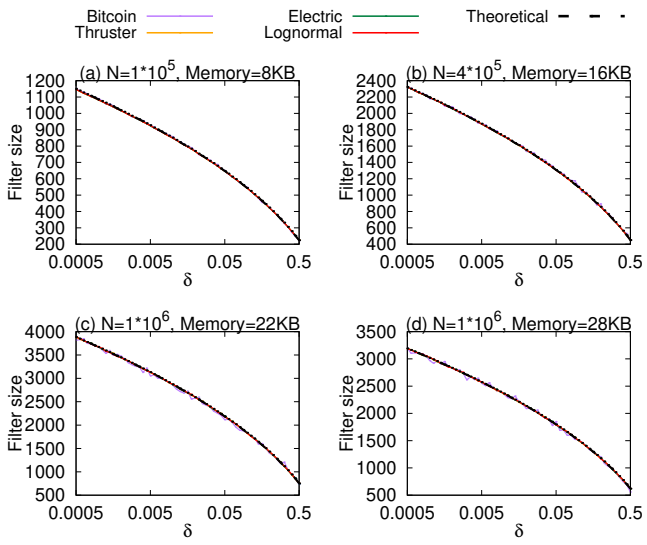

Figure 24: Accurate average filter size in Proposition 3.3

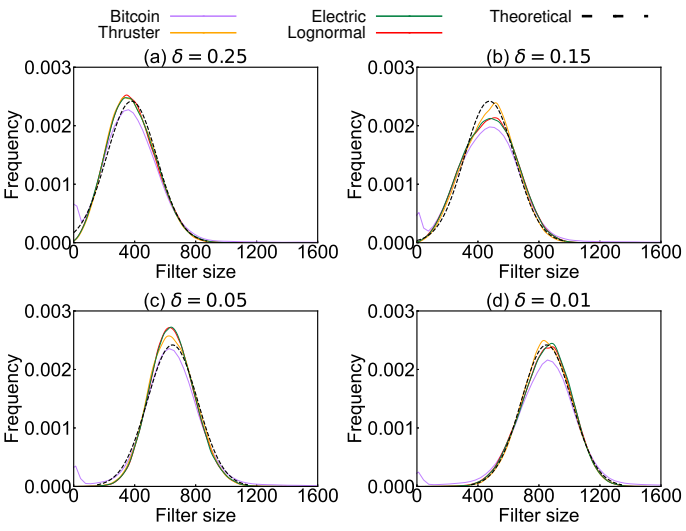

Figure 25: Accurate filter size distribution in Proposition 3.3

$\leq \Pr\left[|f_{\delta'} - \mathbb{E}[f_{\delta'}]| \geq \frac{1}{3}N/(\frac{N}{k})^{\frac{1}{P-1}}\right] \leq \Pr\left[|X| \geq \frac{1}{3}N/(\frac{N}{k})^{\frac{1}{P-1}}\right] \leq \delta'$, given that $f_{\delta'} - \mathbb{E}[f_{\delta'}]$ is σ^2-sub-Gaussian (Proposition 3.3).

With the conclusion of $\sum_{h=1}^{H-1} m_h w_h^2 \leq \frac{2N^2/k^2}{c^3(2c-1)}$ in KLL sketch [24], applying the Chernoff tail bound for the σ^2-sub-Gaussian variable gives $\Pr\left[|X| \geq \frac{1}{3}N/(\frac{N}{k})^{\frac{1}{P-1}}\right] \leq 2\exp\left(\frac{-\left(\frac{1}{3}N/(\frac{N}{k})^{\frac{1}{P-1}}\right)^2}{2\sigma^2}\right) \leq 2\exp\left(\frac{-N^{(2-\frac{2}{P-1})}k^{\frac{2}{P-1}}}{9\sum_{h=1}^{H-1} m_h w_h^2}\right) \leq 2\exp\left(-Ck^{\frac{2P}{P-1}}/N^{\frac{2}{P-1}}\right)$, where $C = c^3(2c-1)/18$ is a constant. To satisfy $2\exp\left(-Ck^{\frac{2P}{P-1}}/N^{\frac{2}{P-1}}\right) \leq \delta' = \frac{\delta}{2(P-1)}$, $k = N^{1/P}(\frac{1}{C}\log\frac{4(P-1)}{\delta})^{\frac{P-1}{2P}}$ is enough and thus the total space cost (analyzed in [26]) does not exceed $\sum_{h=0}^{H-1}(c^h k+2) \leq \frac{k}{1-c} + O(\log N) = O(N^{1/P}\log^{\frac{P-1}{2P}}(\frac{1}{\delta}))$. □

B ADDITIONAL EXPERIMENTS

B.1 Verification of Techniques

B.1.1 Verification of Average Filter Size. We proceed with verifying the average filter size $\mathbb{E}[f_\delta]$, i.e., the number of values lying between $[l_{\phi,\delta}, r_{\phi,\delta}]$ on average, which is essential for pass estimation in Section 3.2. The observed results in four datasets are compared with the theoretical result indicated in Proposition 3.3.

As shown in Figure 24, four kinds of parameters are tested, where the theoretical $\mathbb{E}[f_\delta]$ is very close to the actual statistics in all cases. $\mathbb{E}[f_\delta]$ decreases as δ increases, which is consistent with the intuition of more aggressively shrinking value ranges of the queried quantile.

B.1.2 Verification of Filter Size Distribution. The distribution of f_δ shown in Proposition 3.3, is the base of Formulas 4 and 5 estimating the number of passes. We take many different segments of values in datasets as input for obtaining distributions of filter sizes.

As shown in Figure 25, when N=1 × 10^5 and the space limit is 8KB, real distributions are close to the Gaussian distribution. As δ varies from 0.25 to 0.01, the curves just shift horizontally, i.e., the mean grows while the variance remains unchanged. This is in line with our Proposition 3.3. In dataset Bitcoin, the filter size may be 0, i.e., $l_{\phi,\delta} = r_{\phi,\delta}$ (this case is treated specially). It is owing to duplicated values and thus selection becomes easier. This situation does not affect our method, since the considered δ is below 0.5, i.e., only the right half of the curve is important.

B.2 Performance of System Deployment

B.2.1 Overhead in Data Ingestion. We vary the size of pre-computed synopsis and check the extra overhead. Figure 26 shows the relative space cost on the disk for each dataset, with/without pre-computed sketches, and the relative time cost of ingesting the data under different synopses sizes. The space occupation shows a positive correlation with synopsis size, as expected. The time cost of insertion is almost unchanged for the negligible synopses' construction cost compared to the IO cost in flush as discussed in [1].

B.2.2 Query Performance. We vary the size of pre-computed Page synopsis and report the relative query performance compared to no pre-computation. As shown in Figure 27(a), the relative passes first decrease as synopsis size grows, and remains unchanged when each synopsis is larger than 512Byte. The reason is that the number of passes has reached the lower bound of 2. When the synopsis size exceeds 512Byte, the query time will slightly increase as the cost of merging synopses (total size of pre-computed synopses) increases.

B.2.3 Performance with Updates. We vary the update rate of data on disk and check the performance of query with/without pre-computed synopses. For real datasets we simply update with other values in the dataset, while for the synthetic dataset we update with values sampled from the standard Normal distribution. Figure 28 shows that pre-computed sketch helps significantly, when the data update rate is small. In Section 5.2.2, we merge all synopses even those containing updated values and loose the filter to avoid

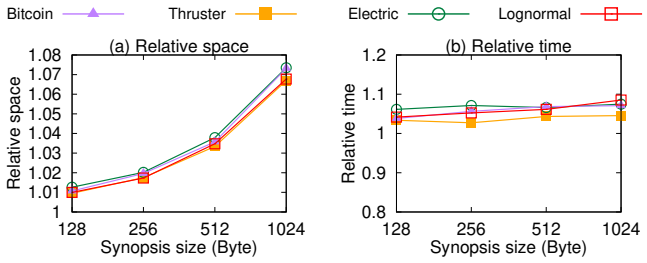

Figure 26: Ingestion performance under various sizes of pre-computed summaries, compared to no pre-computation

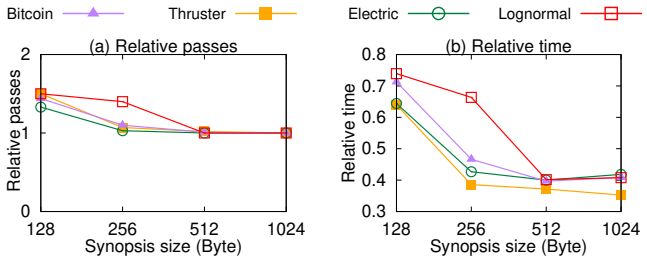

Figure 27: Query performance under various sizes of pre-computed summaries, compared to no pre-computation

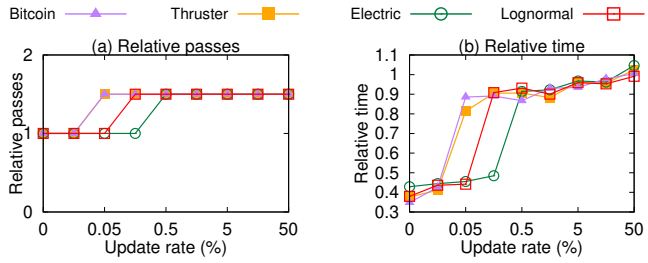

Figure 28: Query performance with pre-computed sketches in various data update rates, compared to no pre-computation

failure. It means that pre-computation will not help much in query when there are many updates. Nevertheless, the out-of-date pre-computed sketches do not harm the overall query performance.